Cooling Model Calibration in a Collaborative Turbine Preliminary Design Process Using the NASA Energy Efficient Engine Part I: 0D Performance Modeling

Patrick Wehrel[1] and Francisco Carvalho[2]

[1]Institute of Propulsion Technology, German Aerospace Center (DLR)
Linder Höhe 1, 51147 Cologne, Germany, patrick.wehrel@dlr.de
[2]Institute of Propulsion Technology, German Aerospace Center (DLR)
Bunsenstraße 10, 37073 Göttingen, Germany, francisco.carvalho@dlr.de

ABSTRACT

Under the NASA Energy Efficient Engine (E3) program, two high pressure turbines (HPTs) were separately developed and tested by General Electric (GE) and Pratt & Whitney (P&W). Despite the corresponding NASA E3 design reports and several subsequent publications related to these HPTs, there is still no uniform and consistent data base, leading to the absence of some essential parameters. Therefore, 0D performance models of the NASA E3 HPTs were generated based on the available literature. The performance results agree well with the literature data and will be presented. Moreover, a well-known turbine cooling modeling approach is calibrated using the 0D performance models and further 1D turbine models, which were created in a collaborative process documented in this work and an accompanying paper. This is crucial, since the predicted coolant mass flows significantly affect the gas turbine efficiency. Based on the obtained calibration results, a simplified turbine cooling model is also derived and calibrated in this paper, being applicable for performance studies in the early phase of preliminary design. In order to quantify the error due to simplification, both the original and the simplified turbine cooling model are applied in two parametric studies.

NOMENCLATURE

A	Area
Bi	Biot Number
c_p	Isobaric Specific Heat Capacity
h	Heat Transfer Coefficient
HLP	Heat Load Parameter
k	Factor in the Simplified Turbine Cooling Model
$\dot{m}$	Mass Flow
R	Reaction
SF	Scaling Factor
St	Stanton Number
T	Temperature
u	Rotor Circumferential Speed
$\Delta T_{abs\text{-}rel}$	Temperature Difference Between Absolute and Relative Coordinate System
δ	Thickness
ε_0	Cooling Effectiveness
ε_f	Film Cooling Effectiveness
η_c	Cooling Efficiency
λ	Thermal Conductivity
ψ	Stage Loading

Subscripts

AF	Airfoil
b	Blade
c	Coolant
coat	Coating
f	Film
g	Gas
in	Inlet
m	Mean, Mid-Section
off	Offtake
out	Outlet
ref	Reference
t	Total
4	Turbine Inlet

Acronyms

ADP	Aerodynamic Design Point
DLR	German Aerospace Center
E3	Energy Efficient Engine
EoF-HD	End of Field at Hot Day Conditions
FPS	Flight Propulsion System
GE	General Electric
GTlab	Gas Turbine Laboratory
HPC	High Pressure Compressor
HPT	High Pressure Turbine
LPT	Low Pressure Turbine
MCL	Maximum Climb
NASA	National Aeronautics and Space Administration
PPI	Performance-PrEDiCT-Interface
P&W	Pratt & Whitney
SAS	Secondary Air System
TBC	Thermal Barrier Coating
TO	Takeoff

Manuscript Received on July 29, 2023
Review Completed on April 16, 2024

INTRODUCTION

In the 1970s, the NASA Energy Efficient Engine (E3) program was started in response to the energy crisis and the sharp rise in fuel prices [1]. The main objective of the program was to develop fuel saving technologies for civil and military transport aircraft engines. General Electric (GE) and Pratt & Whitney (P&W) were each contracted to define a flight propulsion system (FPS) that fulfilled the goals of the NASA E3 program [2, 3]. Based on the respective FPS, GE and P&W separately developed and tested the required engine component technology. Subsequently, the research and test results of GE and P&W were published in a series of in-depth reports. In the field of turbine cooling, GE and P&W's design

reports of the high pressure turbine (HPT) are important, since they contain detailed information on blade designs and cooling systems as well as on the occurring heat transfer coefficients and blade temperatures [4, 5]. The relevance of these reports is also reflected in the fact that they are still cited today and used to validate cooling modeling approaches [6-8]. Despite the abundance of information, the HPT design reports have a significant disadvantage: the data were often published in the form of reduced or nondimensional quantities. This leads to the absence of some essential parameters, which can partially be reconstructed, but this is error prone. To the authors' knowledge, no publication exists to date that consistently presents all of the important data. Therefore, our objective is to model the HPTs of GE and P&W in order to provide a comprehensive data base for future work related to the NASA E3. In this paper, which is Part I of a collaborative series, 0D performance models of the NASA E3 HPTs are presented. These models were generated based on the available literature data. All relevant performance results are attached in this paper. In Part II [9], more detailed 1D turbine models of the NASA E3 HPTs are presented which were created using the 0D performance models as input.

Since the amount of turbine cooling air significantly affects the gas turbine efficiency, it is crucial to use appropriate models that predict the required coolant mass flows already in the early phase of preliminary design. Various cooling models exist in the literature, however, the modeling approach of Holland and Thake [10] has become well-established and has been referenced in other important work [11-14]. By means of the Holland and Thake model, the airfoil coolant mass flows can be estimated row-by-row in the absence of a specific blade geometry or a detailed cooling system. For this purpose, several nondimensional cooling parameters are introduced, such as the cooling efficiency or the film cooling effectiveness, which are required as input. The quantification of these parameters is a challenging task, since they significantly affect the predicted coolant mass flows. In order to facilitate the selection of suitable input parameter values and to provide reliable data, the Holland and Thake cooling model is calibrated in Part II [9] using 1D turbine models of the NASA E3 HPTs. Based on the obtained calibration results, a simplification approach of the Holland and Thake model is presented in this paper. The resulting simplified turbine cooling model is also calibrated by means of the NASA E3 HPT models and can be used in 0D performance calculations to provide a valid prediction of turbine coolant mass flows in the early phase of preliminary design. Finally, the simplified turbine cooling model as well as the original Holland and Thake model are applied in two parametric studies in order to quantify the error due to simplification.

PERFORMANCE MODELING OF THE NASA E3 HPTs

The first step towards the calibration of the Holland and Thake cooling model [10] is the generation of 0D performance models based on the available literature data. For this purpose, the performance module of the framework GTlab (Gas Turbine Laboratory) is applied [15]. The created performance models of the NASA E3 HPTs are presented in Fig. 1 and Fig. 2. All performance results are listed in the appendix, offering a comprehensive data base for future work related to the NASA E3.

P&W's NASA E3 HPT

Fig. 1 illustrates the generated 0D performance model of P&W's one-stage NASA E3 HPT. This model includes a combustor, a secondary air system (SAS) and the high pressure turbine (HPT) itself. The HPT is connected through a shaft to a generator which consumes the turbine power. Air is provided by the SAS to cool the stator and rotor of the HPT.

The aim of the 0D performance model is to reproduce the available literature data of the NASA E3 HPT as accurately as possible. P&W's HPT design report [5] is used as main literary source. If data is missing, the P&W's FPS report [3] is considered. A comparison between the generated performance results and the literature data is presented in the appendix. Important operating points are the aerodynamic design point (ADP), being defined by cruise conditions, and the off-design point takeoff (TO) which is used by P&W to dimension the turbine cooling requirements. The comparison shows that the created performance model reproduces the available literature data of both operating points well.

The assumptions and values used to create the performance model of P&W's one-stage NASA E3 HPT are described in detail for each component below (see also the appendix).

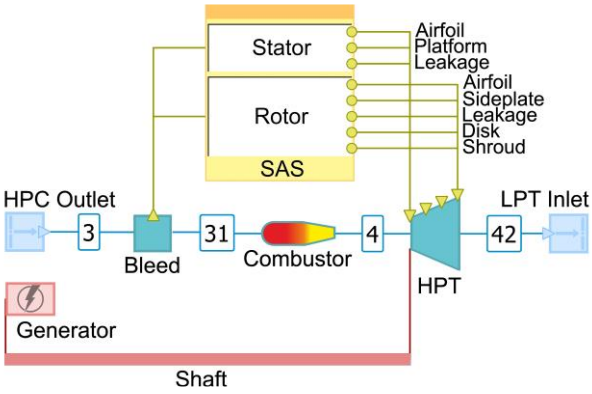

Fig. 1 0D performance model of P&W's one-stage NASA E3 HPT

High Pressure Compressor Outlet. According to the FPS report [3], pressure and temperature are specified in the high pressure compressor (HPC) outlet (station 3) for ADP and TO conditions.

Combustor. Efficiency, pressure loss, inlet pressure, inlet temperature and outlet temperature of P&W's combustor are known from the FPS report [3]. Thus, it is possible to determine the heating value of the fuel used. Subsequently, the combustor setting with the calibrated fuel heating value is applied in the performance model. The HPT inlet temperature (station 4) is set as boundary condition in order to calculate the required fuel mass flow. Note that the combustor outlet temperature at ADP differs between the FPS report [3] and the HPT design report [5].

High Pressure Turbine. The HPT design report [5] contains information on HPT inlet mass flow, pressure ratio and required power which are used as input to generate the ADP. Consequently, the HPC outlet mass flow, the HPT efficiency and the low pressure turbine (LPT) inlet state (station 42) are results of the performance model. The LPT inlet conditions at ADP agree well with P&W's LPT design report [16]. Since the HPT design report [5] does not provide any data on the selected input at TO, it is assumed for simplicity that reduced HPT inlet mass flow, the pressure ratio and the efficiency are equal at ADP and TO. According to the HPT performance data listed in the FPS report [3], this is a valid assumption.

Secondary Air System. Pressure and temperature of stator and rotor cooling air are known at TO from the HPT design report [5]. For ADP modeling, the pressure loss and the specific heating (transferred heat per mass) within the SAS are assumed to be equal to TO conditions. Since the HPT inlet temperature (station 4) and the rotor inlet temperature (station 41) are given in the HPT design report [5], the absolute stator coolant mass flow can be calculated by using mass conservation and the first law of thermodynamics. Subsequently, the computed coolant mass flow and the relative stator coolant mass flow, which is known from the report, are used to determine the reference mass flow of P&W's cooling air design. Finally, it is possible to calculate the absolute rotor coolant mass flow by considering the reference mass flow and the reported relative rotor coolant mass flow. Note that all relative coolant mass

flows are assumed to be constant at all operating points. Regarding cooled turbine performance modeling, it is assumed that rotor cooling air does not generate work within a turbine stage.

Shaft. The HPT design report [5] provides speed data that is applied as performance model input. Moreover, mechanical losses are neglected.

GE's NASA E3 HPT

In contrast to the previously presented performance model of P&W's one-stage NASA E3 HPT, the 0D performance model of GE's NASA E3 HPT is more complex, since the HPT has two stages and a high pressure compressor (HPC) needs to be considered (see Fig. 2). Nevertheless, a similar setup as in Fig. 1 is pursued, but now the HPT is connected to the HPC and an additional turbine stage is considered in the SAS. HPC modeling is based on the HPC reports [17, 18] which contain relevant data and a compressor map shown in the appendix.

As before, the aim of the 0D performance model is to accurately reproduce the available literature data of the NASA E3 HPT. The HPT design report by GE [4] is the main literary source, whereas GE's FPS report [2] is only applied in case of missing data. The comparison between the generated performance results and the literature data is also attached in the appendix. Note that GE's NASA E3 HPT is designed at maximum climb (MCL). Relevant off-design points are takeoff (TO) as well as end of field at hot day conditions (EoF-HD) which is defined by a Mach number of 0.3 at sea level, an ambient temperature of 50 °C and a limited turbine rotor inlet temperature of 1616 K [4]. Since the highest coolant and hot gas temperatures occur at EoF-HD, this operating point is used by GE to dimension the turbine cooling requirements. A good agreement with the available literature data is achieved here as well.

The assumptions and values used to create the performance model of GE's two-stage NASA E3 HPT are described in detail for each component below (see also the appendix).

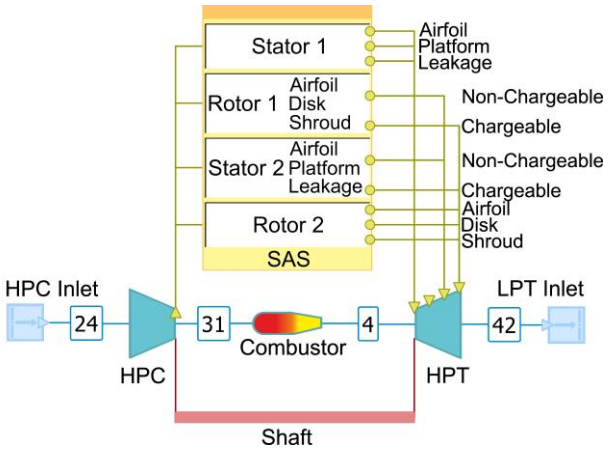

Fig. 2 0D performance model of GE's two-stage NASA E3 HPT

High Pressure Compressor. The HPC is designed at MCL using the inlet conditions, the pressure ratio, the efficiency and the reduced relative speed listed in the FPS report [2] as boundary condition. Thus, the absolute HPC inlet mass flow is a result. For HPC off-design modeling, the compressor map shown in the appendix is applied. Since the selected input parameters for MCL modeling are unknown at TO, they are treated as output parameters and the HPC pressure ratio and overall pressure ratio are specified instead in order to model the TO operating point. Regarding EoF-HD, only HPC outlet pressure and temperature are given in the HPT design report [4], so that HPC inlet conditions are also an output.

Combustor. Efficiency and pressure loss of GE's combustor are listed in the FPS report [2] and are included in the performance model for all operating points. Since the fuel heating value is not known, the fuel heating value of P&W's combustor is assumed. In order to calculate the required fuel mass flow, the HPT rotor inlet temperature (station 41) is specified in all operating points according to the HPT design report [4]. By using mass conservation and the first law of thermodynamics and considering the coolant mass flow of the first HPT stators, the required fuel mass flow and the corresponding HPT inlet temperature are determined.

High Pressure Turbine. The HPT design report [4] provides information on rotor inlet temperature (station 41) and pressure ratio. Moreover, the required turbine power is determined by the HPC which in turn supplies the HPT inlet mass flow. Using these parameters as input, it is possible to create the MCL design point and the LPT inlet state (station 42) results from the performance model. The appendix indicates that the LPT inlet conditions at MCL agree well with GE's LPT design report [19]. For HPT off-design modeling, the rotor inlet temperature is also specified according to the HPT design report [4]. As with the performance model of P&W's NASA E3 HPT, the reduced HPT inlet mass flow, the pressure ratio and the efficiency are assumed to be constant at MCL, TO and EoF-HD due to missing data. Considering the HPT design report [4] and the HPT test results [20], this is also a valid assumption in this case.

Secondary Air System. The relative coolant mass flows of GE's two-stage NASA E3 HPT can be reconstructed at EoF-HD by means of the HPT design report [4] and are assumed to be constant at all operating points. Data is missing only for the first rotor disk cooling, but a realistic value can be estimated considering the known total cooling air demand of the HPT that has to be fulfilled. Since the HPC inlet mass flow (station 24) is used as reference for all relative coolant mass flows and the HPT inlet state results from the performance model, it is possible to calculate all absolute coolant mass flows. First stage cooling air is extracted after the HPC (station 3), whereas second stage cooling air is extracted in the seventh stage of GE's ten-stage NASA E3 HPC. To reproduce this bleed within the HPC of the performance model, the cooling air extraction is located at a relative enthalpy increase of 70 %.

Except for the first stage rotor, the HPT design report [4] contains information on coolant temperatures at EoF-HD. For approximating the first stage rotor coolant temperature, P&W's NASA E3 HPT is referenced and the same temperature difference between extraction (station 3) and injection is assumed. Regarding coolant pressures, values are available in the HPT design report [4] only for the first stage stator at Eof-HD. For all other components, pressure losses within the SAS are not considered due to a lack of data. This has no negative impact on modeling quality, since the GTlab performance module sets the coolant ejection pressure equal to the hot gas pressure anyway. This is done regardless of the pressure loss within the SAS, so coolant pressures in the performance model are rather informative and can be used as input for preliminary design tools with a higher fidelity. In order to determine coolant temperatures and pressures at MCL and TO, pressure losses and the specific heating (transferred heat per mass) within the SAS are assumed to be equal to EoF-HD conditions.

Concerning cooled turbine performance modeling, it is assumed that rotor cooling air does not generate work within a turbine stage. According to the HPT design report [4], the work contribution of the second rotor is 43.5 %. Consequently, it is supposed that 43.5 % of the cooling air of the first rotor and second stator perform work within the HPT (note that the two-stage turbine is modeled as an equivalent single-stage turbine [21, 22]).

Shaft. Speed data is provided by the HPT design report [4] for all operating points. The design speed at MCL is set via the reduced relative speed specification, whereas the speeds at TO and EoF-HD results from the HPC compressor map. Furthermore, low mechanical losses are considered at all operating points.

SIMPLIFIED TURBINE COOLING MODEL

The prediction of the required airfoil coolant mass flows of each blade row in the absence of specific blade geometries or detailed cooling systems is a challenging task in the early phase of preliminary design. Nevertheless, this is an important issue, since coolant mass flows significantly affect the gas turbine efficiency. An appropriate approach for this purpose is the well-known cooling model of Holland and Thake [10], which is based on the idea of Halls [23], who introduced a standard blade with infinite thermal conductivity and thus uniform blade temperature. The Holland and Thake model and its application in a 1D turbine design process is described in detail in Part II of this collaborative series [9]. The essential equation for calculating the relative coolant mass flow $\dot{m}_c/\dot{m}_g$ of a blade row is as follows ($\dot{m}_g$ is the respective blade row inlet mass flow):

$$\frac{\dot{m}_c}{\dot{m}_g} = \frac{c_{p,g}}{c_{p,c}} \cdot \frac{A_b}{A_g} \cdot St_g \cdot HLP \cdot SF \tag{1}$$

$c_{p,g}/c_{p,c}$ is the ratio between the isobaric specific heat capacity of the hot gas and the coolant, A_b/A_g is defined as the ratio between the blade surface area and the hot gas throat area, St_g is the hot gas Stanton number and HLP is the heat load parameter. Since the modeling approach of Holland and Thake only considers the airfoil coolant mass flow $\dot{m}_{c,AF}$, a scaling factor $SF = \dot{m}_c/\dot{m}_{c,AF}$ is used to provide sufficient cooling air for peripheral elements, such as end walls or discs. Realistic scaling factors for turbine stators and rotors can be derived from the NASA E3 HPT design reports [4, 5] and are listed in Table. 2. The heat load parameter HLP is a dimensionless measure of the airfoil cooling requirement and can be calculated by introducing several nondimensional cooling parameters as shown in Eq. (3).These parameters reflect the technology level of the cooling system [24]. The heat load parameter HLP is defined as

$$HLP = \frac{\dot{m}_c c_{p,c}}{A_g h_g} \tag{2}$$

and can be transformed to [12]:

$$HLP = \frac{\varepsilon_f(1-\eta_c)+\varepsilon_0(\varepsilon_f\eta_c-1)}{\eta_c(\varepsilon_0-1)(1+Bi_{coat})} \tag{3}$$

The cooling effectiveness ε_0 is defined in Eq. (4) and depends on the total hot gas temperature $T_{t,g}$, the total coolant inlet temperature $T_{t,c,in}$ and the average blade temperature T_b which is limited by the material used.

$$\varepsilon_0 = \frac{T_{t,g}-T_b}{T_{t,g}-T_{t,c,in}} \tag{4}$$

The cooling efficiency η_c describes the heating of the cooling air within the blade and the film cooling effectiveness ε_f considers the protective effect of the cooling film. Since the total coolant outlet temperature $T_{t,c,out}$ and the film cooling temperature T_f are usually unknown in the early phase of preliminary design, the cooling efficiency η_c and the film cooling effectiveness ε_f are treated as input parameters in the Holland and Thake model and have to be quantified appropriately. To provide indicative values for the quantification, these parameters are calibrated in Part II [9] using 1D turbine models of the NASA E3 HPTs.

$$\eta_c = \frac{T_{t,c,out}-T_{t,c,in}}{T_b-T_{t,c,in}} \tag{5}$$

$$\varepsilon_f = \frac{T_{t,g}-T_f}{T_{t,g}-T_{t,c,out}} \tag{6}$$

In case of coated blades, the coating Biot number Bi_{coat} has to be included in Eq. (3) in order to account for the insulating effect of a thermal barrier coating (TBC).

$$Bi_{coat} = \frac{h_g \delta_{coat}}{\lambda_{coat}} \tag{7}$$

Since the area ratio A_b/A_g and the hot gas Stanton number St_g in Eq. (1) are usually not known in the early phase of preliminary design, the cooling model of Holland and Thake cannot be applied in 0D performance studies. Therefore, the simplification of the model is proposed by introducing a factor $k = A_b/A_g \cdot St_g$ that is calibrated in this paper using the generated NASA E3 HPT models.

$$\frac{\dot{m}_c}{\dot{m}_g} = \frac{c_{p,g}}{c_{p,c}} \cdot k \cdot HLP \cdot SF \tag{8}$$

When calculating the heat load parameter HLP in performance analyses, it is recommended to apply calibrated nondimensional cooling parameters, except for the cooling effectiveness ε_0 which can be determined if a permissible average blade temperature is given. This is trivial for stators, but for rotors the total hot gas temperature $T_{t,g}$ in the relative coordinate system has to be considered in Eq. (4) which is usually not known in 0D performance studies. The temperature drop between absolute and relative coordinate system $\Delta T_{abs\text{-}rel}$ depends mainly on the rotor circumferential speed u, but also on turbine stage design parameters, such as reaction R and stage loading ψ [25, 26]. If neither the reaction nor the stage loading is known in the early phase of preliminary design, the relevant parameters of the generated 1D NASA E3 HPT models [9] are presented in Table. 1 as orientation. Note that all parameters are determined in the turbine mid-section.

Table. 1 Mean temperature difference between absolute and relative coordinate system $\Delta T_{abs\text{-}rel,m}$ of the 1D turbine models of the NASA E3 HPTs [9] at takeoff conditions

Stage	R_m [-]	ψ_m [-]	u_m [m/s]	$\Delta T_{abs\text{-}rel,m}$ [K]
P&W HPT Rotor 1	0.39	1.60	556	214
GE HPT Rotor 1	0.32	1.38	474	151
GE HPT Rotor 2	0.31	1.06	476	129

COUPLED PERFORMANCE AND TURBINE MODELING

After deriving the simplified turbine cooling model (see Eq. (8)), which can be applied directly in performance studies, this section introduces a method to incorporate the original Holland and Thake cooling approach (see Eq. (1)) in 0D performance models. In addition to the performance module, the framework GTlab also includes a 1D turbine preliminary design tool called PrEDiCT [27]. As illustrated in Fig. 3, the performance module and PrEDiCT can be connected via the Performance-PrEDiCT-Interface (PPI), enabling coupled 0D performance and 1D turbine modeling [28]. The PPI transfers the necessary input parameters, such as turbine inlet and coolant conditions, power requirements and shaft speeds, to PrEDiCT and executes it. Subsequently, PrEDiCT provides the calculated coolant mass flows and turbine efficiency to the performance module which is also executed. This results in a closed loop that is iterated by the PPI until the turbine power deviation between the performance module and PrEDiCT is less than 0.001%. Since the original model of Holland and Thake is integrated in PrEDiCT for coolant flow calculations, the PPI enables the use of the original cooling approach in 0D performance models. However, this is far more complex than applying the simplified turbine cooling model.

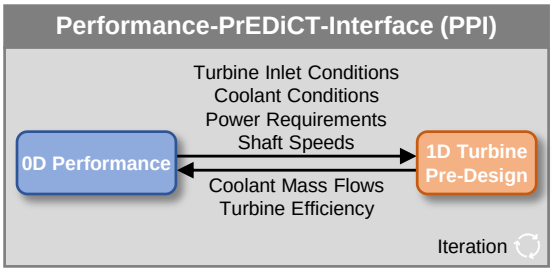

Fig. 3 Functionality of the Performance-PrEDiCT-Interface (PPI)

RESULTS AND DISCUSSION

In this section, the previously derived simplified turbine cooling model is calibrated based on the generated NASA E3 HPT models. Additionally, the turbine inlet temperature and the coolant temperature are varied separately in two parametric studies in order to quantify the error due to simplification. Therefore, the simplified turbine cooling model (see Eq. (8)) is used directly in the 0D performance model, whereas the original Holland and Thake model (see Eq. (1)) is applied by means of the coupled performance and turbine modeling approach presented above. Assuming a constant cooling efficiency η_c and film cooling effectiveness ε_f, the cooling effectiveness ε_0 and the heat load parameter *HLP* can be calculated depending on total hot gas temperature $T_{t,g}$ and the total coolant inlet temperature $T_{t,c,in}$ (see Eq. (3) and Eq. (4)).

Calibration of the Simplified Turbine Cooling Model

Based on GE's and P&W's HPT design reports [4, 5], the relative coolant mass flow $\dot{m}_c/\dot{m}_g$ and the occurring average blade temperature T_b of each blade row can be reproduced. Thus, a calibration of the nondimensional cooling parameters of the Holland and Thake model [10] is possible which is the objective of this collaborative series. The cooling model calibration is crucial, since the predicted coolant mass flows significantly affect the gas turbine efficiency.

As a valid calibration basis, 0D performance models (see Fig. 1 and Fig. 2) and more detailed 1D turbine models (see [9]) of the NASA E3 HPTs were generated using the available literature data. In Part II [9], all required input parameters of the original Holland and Thake equation are calibrated (see Eq. (1)). The calibration target parameter is the known relative coolant mass flow $\dot{m}_c/\dot{m}_g$ which is matched for each blade row. Since film-cooled blade rows require the cooling efficiency η_c and the film cooling effectiveness ε_f as input (see Eq. (3)), this is only possible if one of these two parameters is predefined. Accordingly, the cooling efficiency η_c is calibrated, whereas the film cooling effectiveness ε_f is set. In order to provide a range of valid η_c-ε_f-combinations, the calibration is carried out in [9] for a film cooling effectiveness ε_f of 0.15, 0.20, 0.25 and 0.30.

Using the results of [9], the calibration of the previously derived simplified turbine cooling model (see Eq. (8)) is pursued in this paper in order to provide a suitable cooling prediction approach for performance studies in the early phase of preliminary design. Hence, the introduced factor $k = A_b/A_g \cdot St_g$ has to be determined which is carried out in Table. 2 at takeoff conditions. Note that Table. 2 presents the results for a film cooling effectiveness ε_f of 0.20, but this only influences the calibration of the cooling efficiency η_c. All other nondimensional cooling parameters of the Holland and Thake model (see Eq. (1)), such as the area ration A_b/A_g or the hot gas Stanton number St_g, are not affected by the η_c-ε_f-calibration because they are determined directly in [9] on the basis of the NASA E3 HPT design reports [4, 5] and the corresponding 0D performance and 1D turbine models. Consequently, the calculated *k*-factors are also independent of the η_c-ε_f-combinations.

When differentiating between stators and rotors, the *k*-factors are close together, although the NASA E3 HPT models were created independently based on the literature data. For stators, *k* is in the range of 0.023 to 0.029 (0.023 to 0.026 for first stage stators), whereas *k* is between 0.015 and 0.019 for rotors (0.018 and 0.019 for first stage rotors). When comparing the *k*-factors of the first stage stators and rotors between P&W's and GE's NASA E3 HPT, it can be observed that the respective *k*-factors are similar, despite a discrepancy in area ratio A_b/A_g and hot gas Stanton number St_g. Apparently, a lower area ratio A_b/A_g is related to a higher hot gas Stanton number St_g, resulting in similar *k*-factors.

Table. 2 Calibration of the k-factor of the simplified turbine cooling model at takeoff conditions

Parameter	P&W		GE				Source
	Stage 1		Stage 1		Stage 2		
	Stator	Rotor	Stator	Rotor	Stator	Rotor	
η_c [-]	0.475	0.511	0.468	0.281	0.979	0.472	[9]
ε_f [-][a)]	0.200	0.200	0.200	0.200	0	0	[9]
ε_0 [-]	0.616	0.500	0.649	0.450	0.250	0.188	[9]
T_b [K]	1179	1122	1155	1179	1185	1131	[9]
Bi_{coat} [-]	No TBC[b)]		No TBC[b)]				[9]
HLP [-]	2.486	1.375	2.935	1.818	0.341	0.490	[9]
$c_{p,g}/c_{p,c}$ [-]	1.121	1.095	1.117	1.099	1.107	1.062	
A_b/A_g [-]	21.08	11.14	11.91	7.054	13.98	5.103	[9]
St_g [10^3]	1.254	1.715	1.944	2.515	2.100	2.845	[9]
SF [-]	1.345	1.876	1.530	1.850	1.230	2.320	[9]
$\dot{m}_c/\dot{m}_g$ [-]	0.099	0.054	0.116	0.066	0.014	0.018	
k [-]	0.026	0.019	0.023	0.018	0.029	0.015	

a) Predefined input parameter in [9].
b) In the HPT design reports [4, 5], no proper TBCs were used, but a kind of precursor to them (e. g. PWA 286 [29]). These coatings were applied for oxidation and erosion resistance rather than for thermal insulation and are therefore neglected in cooling air modeling.

Variation of Turbine Inlet Temperature

In the 0D performance model of P&W's one-stage NASA E3 HPT (see Fig. 1), the total turbine inlet temperature $T_{t,g,4}$ is varied by ±10 % at takeoff conditions. The total coolant inlet temperature $T_{t,c,in}$ is fixed in this parametric study. Fig. 4 shows the effect on the required coolant mass flow $\dot{m}_c$ using the literature-based performance data listed in the appendix as well as the calibration results and the calculated *k*-factors presented in Table. 2 as reference configuration. If the total turbine inlet temperature is increased, the stator coolant mass flow is underestimated by the simplified cooling model. In the case investigated here, the reason for this is the assumption of a constant *k*-factor which increases in the original cooling model due to a growing area ratio A_b/A_g and hot gas Stanton number St_g. Regarding rotor coolant mass flow, the same relations occur, but in this case the error due to a constant *k*-factor is compensated by an overestimated heat load parameter *HLP*. Since the simplified cooling model underestimates the stator coolant mass flow, the rotor inlet temperature and thus the cooling effectiveness ε_0 are greater than in the original cooling model. Consequently, the heat load parameter of the rotor is calculated too high in the simplified cooling model, leading to a pseudo increase in *k*-factor. Hence, the predictions of both modeling approaches are quite similar in the rotor case. If the total turbine inlet temperature is reduced, the opposite trends can be observed in Fig. 4.

Variation of Coolant Temperature

Retaining a constant total combustor inlet temperature (station 31 in Fig. 1) and total turbine inlet temperature $T_{t,g,4}$, the total coolant offtake temperature $T_{t,c,off}$ (temperature at the bleed extraction) is varied by ±10 % at takeoff conditions in the 0D performance model of P&W's one-stage NASA E3 HPT (see Fig. 1). This leads to a variation in stator and rotor total coolant inlet

temperature $T_{t,c,in}$, the effect on the required coolant mass flow $\dot{m}_c$ is presented in Fig. 5. Again, the literature-based performance data listed in the appendix as well as the calibration results and the calculated k-factors shown in Table. 2 serve as reference configuration. Since the area ratio A_b/A_g and the hot gas Stanton number St_g of the stator and thus the k-factor are only affected marginally by the coolant temperature, the simplified and the original cooling model predict similar stator coolant mass flows. Consequently, the rotor inlet temperature is almost equal in both approaches. As for the stator, the discrepancy in the k-factor is also small for the rotor, so that the simplified and the original cooling model estimate similar rotor coolant mass flows.

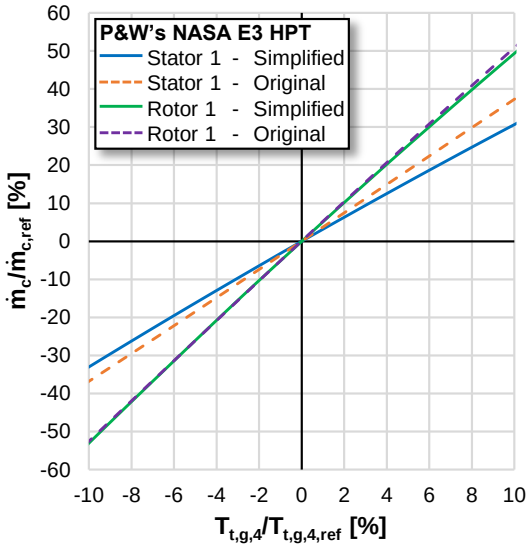

Fig. 4 Variation of turbine inlet temperature $T_{t,g,4}$ at takeoff conditions

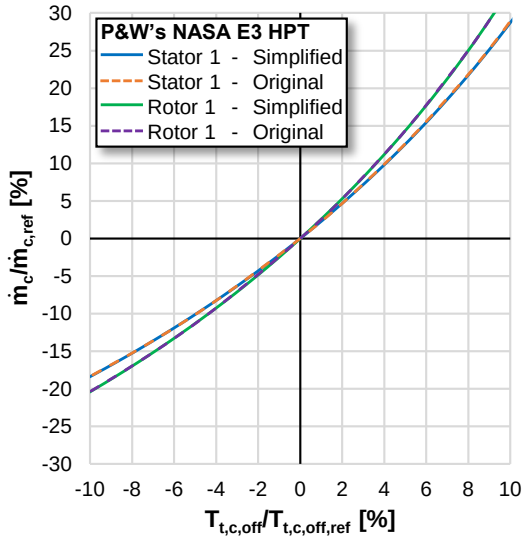

Fig. 5 Variation of coolant offtake temperature $T_{t,c,off}$ at takeoff conditions

CONCLUSION

As part of the NASA Energy Efficient Engine (E3) program, both General Electric (GE) and Pratt & Whitney (P&W) developed and tested a high pressure turbine (HPT). The corresponding HPT design reports are still cited today and used for validation, indicating their importance and popularity. Despite the abundance of information, some essential parameters are missing in the HPT design reports, leading to a lack of a uniform and consistent data base. Therefore, 0D performance models of the NASA E3 HPTs were generated based on the available literature whose results agree well with the literature data. Thus, this paper provides a comprehensive data base for all future work related to the NASA E3.

Based on a well-known cooling modeling approach, this paper also derives a simplified turbine cooling model which is suitable for performance studies in the early phase of preliminary design. In this work and an accompanying paper [9], the input parameters of the original and the simplified cooling model are calibrated for each blade row of the NASA E3 HPTs using the information on the relative coolant mass flows and the occurring blade temperatures provided in the NASA E3 HPT design reports. The cooling model calibration is crucial, since the calculated coolant mass flows significantly affect the gas turbine efficiency. Thus, the use of uncalibrated cooling models could lead to incorrect predictions and should be avoided. If a reliable calibrated reference point has been determined, either the original or the simplified cooling model can be applied. Both modeling approaches largely predict similar coolant mass flows for narrow parameter variations which is demonstrated in this paper by conducting two parametric studies. Since the simplified cooling model is more user-friendly and mostly provides comparable predictions to the original cooling model, it is particularly applicable for performance studies in the early phase of preliminary design, insofar as a reliable calibrated reference point is available.

ACKNOWLEDGEMENTS

This work is supported by the DLR and was executed within the project Future Fighter Engine Technologies FFE+. We sincerely thank all project participants for their support.

REFERENCES

[1] Ciepluch, C. C., Davis, D. Y., and Gray, D. E., 1987, "Results of NASA's Energy Efficient Engine Program," *Journal of Propulsion and Power*, Vol. 3, No.6, pp.560-568.

[2] Davis, D. Y., and Stearns, E. M., 1985, "NASA Energy Efficient Engine - Flight Propulsion System Final Design and Analysis," *General Electric Report NASA CR-168219,* NASA Lewis Research Center, Cleveland, OH.

[3] Bisset, J. W., and Howe, D. C., 1983, "NASA Energy Efficient Engine - Flight Propulsion System Preliminary Analysis and Design Report - Final Update," *Pratt & Whitney Report NASA CR-174701,* NASA Lewis Research Center, Cleveland, OH.

[4] Halila, E. E., Lenahan, D. T., and Thomas, T. T., 1982, "NASA Energy Efficient Engine - High Pressure Turbine Test Hardware Detailed Design Report," *General Electric Report NASA CR-167955,* NASA Lewis Research Center, Cleveland, OH.

[5] Thulin, R. D., Howe, D. C., and Singer, I. D., 1982, "NASA Energy Efficient Engine - High-Pressure Turbine Detailed Design Report," *Pratt & Whitney Report NASA CR-165608,* NASA Lewis Research Center, Cleveland, OH.

[6] Apostolidis, A., 2015, "Turbine Cooling and Heat Transfer Modelling for Gas Turbine Performance Simulation," *Ph.D. Thesis*, School of Engineering, Cranfield University, Cranfield, United Kingdom.

[7] Chowdhury, N. H. K., Zirakzadeh, H., and Han, J. C., 2017, "A Predictive Model for Preliminary Gas Turbine Blade Cooling Analysis," *ASME Journal of Turbomachinery*, Vol. 139, No. 9.

[8] Yin, F., Tiemstra, F. S., and Rao, A. G., 2018, "Development of a Flexible Turbine Cooling Prediction Tool for Preliminary Design of Gas Turbines," *ASME Journal of Engineering for Gas Turbines and Power*, Vol. 140, No. 9.

[9] Carvalho, F., Wehrel, P., Grunwitz, C., Schöffler, R., and Brakmann, R. G., 2023, "Cooling Model Calibration in a Collaborative Turbine Preliminary Design Process Using the NASA Energy Efficient Engine - Part II: 1D Turbine Modeling," *International Journal of Gas Turbine, Propulsion*

and Power Systems.

[10] Holland, M. J., and Thake, T. F., 1980, "Rotor Blade Cooling in High Pressure Turbines," *Journal of Aircraft*, Vol. 17, No. 6, pp.412-418.

[11] Horlock, J. H., Watson, D. T., and Jones, T. V., 2001, "Limitations on Gas Turbine Performance Imposed by Large Turbine Cooling Flows," *ASME Journal of Engineering for Gas Turbines and Power*, Vol. 123, No. 3, pp.487-494.

[12] Young, J. B., and Wilcock, R. C., 2002, "Modeling the Air-Cooled Gas Turbine: Part 2 - Coolant Flows and Losses," *ASME Journal of Turbomachinery*, Vol. 124, No. 2, pp.214-221.

[13] Wilcock, R. C., Young, J. B., and Horlock, J. H., 2005, "The Effect of Turbine Blade Cooling on the Cycle Efficiency of Gas Turbine Power Cycles," *ASME Journal of Engineering for Gas Turbines and Power*, Vol. 127, No. 1, pp.109-120.

[14] Torbidoni, L., and Horlock, J. H., 2005, "A New Method to Calculate the Coolant Requirements of a High-Temperature Gas Turbine Blade," *ASME Journal of Turbomachinery*, Vol. 127, No. 1, pp.191-199.

[15] Reitenbach, S., Vieweg, M., Becker, R., Hollmann, C., Wolters, F., Schmeink, J., Otten, T., and Siggel, M., 2020, "Collaborative Aircraft Engine Preliminary Design using a Virtual Engine Platform, Part A: Architecture and Methodology," *AIAA Scitech 2020 Forum*, Orlando, FL.

[16] Leach, K., Thulin, R., and Howe, D., 1982, "NASA Energy Efficient Engine - Turbine Intermediate Case and Low-Pressure Turbine Component Test Hardware Detailed Design Report," *Pratt & Whitney Report NASA CR-167973,* NASA Lewis Research Center, Cleveland, OH.

[17] Holloway, P. R., Knight, G. L., Koch, C. C., and Shaffer, S. J, 1982, "NASA Energy Efficient Engine - High Pressure Compressor Detailed Design Report," *General Electric Report NASA CR-16558,* NASA Lewis Research Center, Cleveland, OH.

[18] Cline, S. J., Fesler, W., Liu, H. S., Lovell, R. C., and Shaffer, S. J., 1983, "NASA Energy Efficient Engine - High Pressure Compressor Component Performance Report," *General Electric Report NASA CR-168245,* NASA Lewis Research Center, Cleveland, OH.

[19] Cherry, D. G., Gay, C. H., and Lenahan, D. T., 1983, "NASA Energy Efficient Engine - Low Pressure Turbine Test Hardware Detailed Design Report," *General Electric Report NASA CR-167956,* NASA Lewis Research Center, Cleveland, OH.

[20] Timko, L. P., 1984, "NASA Energy Efficient Engine - High Pressure Turbine Component Test Performance Report," *General Electric Report NASA CR-168289,* NASA Lewis Research Center, Cleveland, OH.

[21] Walsh, P. P., and Fletcher, P., 2004, *Gas Turbine Performance*, Blackwell Science, Oxford, pp.226-229.

[22] Kurzke, J., and Halliwell, I., 2018, *Propulsion and Power – An Exploration of Gas Turbine Performance Modeling*, Springer Nature, Cham, pp.670-677.

[23] Halls, G. A., 1967, "Air Cooling of Turbine Blades and Vanes - An Account of the History and Development of Gas Turbine Cooling," *Aircraft Engineering and Aerospace Technology*, Vol. 39, No. 8, pp.4-14.

[24] Town, J., Straub, D., Black, J., Thole, K. A., and Shih, T. I-P., 2018, "State-of-the-Art Cooling Technology for a Turbine Rotor Blade," *ASME Journal of Turbomachinery*, Vol. 140, No. 7.

[25] Bräunling, W. J. G., 2015, *Flugzeugtriebwerke - Grundlagen, Aero-Thermodynamik, Ideale und reale Kreisprozesse, Thermische Turbomaschinen, Komponenten, Emissionen und Systeme*, Springer-Verlag, Berlin, Heidelberg, pp.1312-1316.

[26] Dixon, S. L., and Halls, C. A., 2013, *Fluid Mechanics and Thermodynamics of Turbomachinery*, Elsevier Inc., Amsterdam, pp.119-168.

[27] Grunwitz, C., Nelles, D., Carvalho, F., Schöffler, R., Brose, N., and Wehrel, P., 2023, "A Comprehensive Multifidelity Design and Analysis Process for Cooled Axial Flow Turbines: From Concept to Component," *International Journal of Gas Turbine, Propulsion and Power Systems*.

[28] Wehrel, P., Schöffler, R., Grunwitz, C., Carvalho, F., Plohr, M., Häßy, J., and Petersen, A., 2023, "Performance and Emissions Benefits of Cooled Ceramic Matrix Composite Vanes for High-Pressure Turbines," *ASME Journal of Engineering for Gas Turbines and Power*, Vol. 145, No. 12.

[29] Swanson, G. A., Linask, I., Nissley, D. M., Norris, P. P, Meyer, T. G., and Walker, K. P., 1987, "Life Prediction and Constitutive Models for Engine Hot Section Anisotropic Materials Program – Second Annual Status Report," *NASA CR-179594,* NASA Lewis Research Center, Cleveland, OH.

APPENDIX

Nomenclature

FAR	Fuel to Air Ratio
FHV	Fuel Heating Value
h	Specific Enthalpy
$\dot{m}$	Mass Flow
n	Rotational Speed
OPR	Overall Pressure Ratio
p	Pressure
P	Power
T	Temperature
η	Efficiency

Subscripts

AF	Airfoil
c	Coolant
comb	Combustion
D	Disk
DP	Design Point
in	Inlet
is	Isentropic
L	Leakage
mech	Mechanical
out	Outlet
PF	Platform
red	Reduced
ref	Reference
rel	Relative
std	Standard
Sh	Shroud
SP	Sideplate
t	Total
virt	virtual
24	High Pressure Compressor Inlet
41	High Pressure Turbine Rotor Inlet
415	High Pressure Turbine Rotor Outlet

Acronyms

ADP	Aerodynamic Design Point
EoF-HD	End of Field at Hot Day Conditions
E3	Energy Efficient Engine
GE	General Electric
HPC	High Pressure Compressor
HPT	High Pressure Turbine
ICAO	International Civil Aviation Organization
LPT	Low Pressure Turbine
MCL	Maximum Climb
NASA	National Aeronautics and Space Administration
P&W	Pratt & Whitney
SAS	Secondary Air System
TO	Takeoff
ΔT_{ISA}	Temperature Deviation from ICAO Standard Atmosphere

Performance model results of P&W's E3 HPT

			0D Performance Model		Literature		
Component	**Parameter**	**Unit**	**ADP** (Design)	**TO** (Off-Design)	**ADP** (Design)	**TO** (Off-Design)	**Source**
Ambient Conditions	Altitude	m	10668	0	10668	0	[3] Tab. 3
	Mach	-	0.8	0	0.8	0	
	ΔT_{ISA}	K	0	13.9	0	13.9	
HPC Outlet (Station 3 in Fig. 1)	$\dot{m}$	kg/s	30.92	67.59	-	-	-
	p_t	bar	14.0	31.4	-	-	-
	T_t	K	754.15	844.15	754.1	843.15	[3] Tab. 15

Combustor Inlet (Station 31 in Fig. 1)	$\dot{m}$	kg/s	26.59	58.14	-	-	-
	p_t	bar	14.0	31.4	14.0[a)]	31.4[a)]	[3] Tab. 18
	T_t	K	754.15	844.15	754.1	844.15	[3] Tab. 18
Combustor	FAR	-	0.02646	0.02647	see b)	see b)	-
	FHV	MJ/kg	42.6	42.6	-	-	-
	$p_{t,in}/p_{t,out}$	-	0.9450	0.9442	0.9450	0.9442	[3] Tab. 18
	η_{comb}	-	0.9995	0.9995	0.9995	0.9995	[3] Tab. 18
HPT Inlet (Station 4 in Fig. 1)	$\dot{m}$	kg/s	27.30	59.68	27.30[c)]	-	[5] Tab. 4.1-I
	p_t	bar	13.2	29.6	13.2	-	
	T_t	K	1633	1708.15	1633	1708	
HPT	P	MW	14.12	32.41	14.12[d)]	-	[5] Tab. 4.1-I
	$p_{t,in}/p_{t,out}$	-	4.0	4.0	4.0	-	
	$T_{t,41}$	K	1561	1637	1561	1641	
	η_{is}	-	0.8851[e)]	0.8851[e)]	0.8790[f)]	-	
LPT Inlet (Station 42 in Fig. 1)	$\dot{m}$	kg/s	31.62	69.13	31.85[c)]	-	[16] Tab. 4.1-I
	p_t	bar	3.0	6.8	3.2	-	
	T_t	K	1161	1223	1161	-	
SAS	$\dot{m}_{ref}$[g)]	kg/s	31.37	68.59	-	-	-
	$\dot{m}_{c,rel}$	%	13.78	13.78	-	13.78[h)]	[5] Tab. 6.2-I
SAS Stator	$\dot{m}_c$	kg/s	2.70	5.89	-	-	-
	$\dot{m}_{c,rel}$	%	8.62	8.62	-	8.62	[5] Tab. 6.2-I
	$\dot{m}_{c,rel,AF}$	%	6.41	6.41	-	6.41	[5] Tab. 6.2-I
	$\dot{m}_{c,rel,PF}$	%	0.81	0.81	-	0.81	[5] Tab. 6.2-I
	$\dot{m}_{c,rel,L}$	%	1.40	1.40	-	1.40	[5] Tab. 6.2-I
	$p_{t,c,in}$	bar	13.6	30.4	-	-	[5] page 32[i)]
	$T_{t,c,in}$	K	760	850.15	-	850.15	[5] page 32
SAS Rotor	$\dot{m}_c$	kg/s	1.62	3.53	-	-	-
	$\dot{m}_{c,rel}$	%	5.16	5.16	-	5.16	[5] Tab. 6.2-I
	$\dot{m}_{c,rel,AF}$	%	2.75	2.75	-	2.75	[5] Tab. 6.2-I
	$\dot{m}_{c,rel,SP}$	%	0.19	0.19	-	0.19	[5] Tab. 6.2-I
	$\dot{m}_{c,rel,L}$	%	0.23	0.23	-	0.23	[5] Tab. 6.2-I
	$\dot{m}_{c,rel,D}$	%	1.00	1.00	-	1.00	[5] Tab. 6.2-I
	$\dot{m}_{c,rel,Sh}$	%	0.99	0.99	-	0.99	[5] Tab. 6.2-I
	$p_{t,c,in}$	bar	7.9	17.8	-	-	[5] page 41[i)]
	$T_{t,c,in}$	K	739	829.15	-	829.15	[5] page 41
Shaft	n	1/s	220.53	231.1	220.53	231.1	[5] Tab. 4.1-I
	η_{mech}	-	1	1	-	-	-

a) Report unit is psi.

b) Not comparable due to a higher combustor exit temperature at ADP in the HPT design report [5].

c) Mass flow is calculated using the parameter $W\sqrt{T_T}/P_T$. The resulting unit is lbm/s and is converted to kg/s.

d) Report unit is Btu/sec.

e) η_{is} is defined as $\frac{h_{t,41}-h_{t,415}}{h_{t,41}-h_{t,415,is}}$ for one-stage turbines. Stator cooling air (non-chargeable) is ejected isobarically upstream of the rotor to calculate $T_{t,41}$. Rotor cooling air (chargeable) is ejected isobarically downstream of the rotor.

f) Cooled turbine efficiency definition is not known.

g) Reference mass flow for the relative coolant mass flows $\dot{m}_{c,rel}$ of the SAS (named engine airflow w_{ae} in the HPT design report [5]). Virtual parameter in the 0D performance model shown in Fig. 1.

h) Calculated without the portions “Active Clearance” and “Flange Leakage”.

i) Only static pressure given.

Performance model results of GE's E3 HPT

			0D Performance Model			Literature			
Component	**Parameter**	**Unit**	**MCL** (Design)	**TO** (Off-Design)	**EoF-HD** (Off-Design)	**MCL** (Design)	**TO** (Off-Design)	**EoF-HD** (Off-Design)	**Source**
Ambient Conditions	Altitude	m	10668	0	0	10668	0	0	[2] Tab. III [4] Tab. VIII
	Mach	-	0.8	0	0.3	0.8	0	0.3	
	ΔT_{ISA}	K	10	15	35	10	15	35	
HPC Inlet (Station 24 in Fig. 2)	$\dot{m}$	kg/s	31.57	73.10	59.35	31.57[a)]	-	-	[2] Tab. XIV
	p_t	bar	0.6	1.6	1.5	0.6	-	-	
	T_t	K	305	342	367	305	-	-	
HPC	$\dot{m}_{red,std}$	kg/s	54.40	49.39	44.52	54.40	-	-	[2] Tab. XIV
	$n_{red,rel}$	-	0.984	0.964	0.945	0.984	-	-	[2] Tab. XIV
	OPR	-	38.3	32.4	24.7	38.4	32.4	-	[2] Tab. XII
	P	MW	16.02	38.62	31.30	-	-	-	
	$p_{t,out}/p_{t,in}$	-	23.0	20.1	17.4	23.0	20.1	-	[2] Tab. XIV [17] Tab. IX
	η_{is}	-	0.8600	0.8647	0.8647	0.8600	-	-	[2] Tab. XIV
Bleed 2nd HPT Stage	$\dot{m}$	kg/s	0.98	2.27	1.85	-	-	-	-
	p_t	bar	7.1	17.1	14.1	-	-	-	-
	T_t	K	653	702	725	-	-	-	-
HPC Outlet (Station 3 in Fig. 2)	$\dot{m}$	kg/s	30.58	70.82	57.50	-	-	-	-
	p_t	bar	13.9	32.8	26.6	-	-	26.6	[4] Tab. VIII
	T_t	K	795	848	870.15	-	-	870.15	[4] Tab. VIII
Combustor Inlet (Station 31 in Fig. 2)	$\dot{m}$	kg/s	25.61	59.30	48.15	-	-	-	-
	p_t	bar	13.9	32.8	26.6	-	-	-	-
	T_t	K	795	848	870.15	-	-	-	-
Combustor	FAR	-	0.02542	0.02602	0.02522	-	-	-	-
	FHV	MJ/kg	42.6	42.6	42.6	-	-	-	-
	$p_{t,in}/p_{t,out}$	-	0.9500	0.9500	0.9500	0.9500	-	-	[2] Tab. XVI
	η_{comb}	-	0.9990	0.9990	0.9990	0.9990	-	-	[2] Tab. XVI
HPT Inlet (Station 4 in Fig. 1)	$\dot{m}$	kg/s	26.26	60.85	49.36	-	-	-	-
	p_t	bar	13.2	31.2	25.3	-	-	-	-
	T_t	K	1636	1698	1694	-	-	-	-

HPT	$\dot{m}_{41}$	kg/s	29.31	67.92	55.10	28.92[b)]	66.90[b)]	-	[4] Tab. I
	P	MW	16.03	38.66	31.33	-	-	-	-
	$p_{t,in}/p_{t,out}$	-	4.7	4.7	4.7	4.7	-	-	[4] Tab. 3
	$T_{t,41}$	K	1557	1618	1616	1557	1618	1616	[4] Tab. I [4] Tab. VIII
	$T_{t,41,virt}$	K	1532	1593	1592	-	-	-	-
	η_{is}	-	0.9191[c)]	0.9191[c)]	0.9191[c)]	0.9240[d)]	0.9210[d)]	-	[4] Tab. I
LPT Inlet (Station 42 in Fig. 1)	$\dot{m}$	kg/s	32.22	74.64	60.56	-	-	-	-
	p_t	bar	2.8	6.6	5.3	-	-	-	-
	T_t	K	1085	1132	1131	1083	1129	1132.15	[19] Tab. I [19] Tab. IV
SAS	$\dot{m}_{ref} = \dot{m}_{24}$	kg/s	31.57	73.10	59.35	-	-	-	-
	$\dot{m}_{c,rel}$	%	18.87	18.87	18.87	-	-	18.87	[4] Tab. VII
SAS Stator 1	$\dot{m}_c$	kg/s	3.05	7.07	5.74	-	-	-	-
	$\dot{m}_{c,rel}$	%	9.67	9.67	9.67	-	-	-	-
	$\dot{m}_{c,rel,AF}$	%	6.30	6.30	6.30	-	-	6.30	[4] Tab. IX
	$\dot{m}_{c,rel,PF}$	%	2.80	2.80	2.80	-	-	2.80	[4] Tab. IX
	$\dot{m}_{c,rel,L}$	%	0.57	0.57	0.57	-	-	0.57	[4] Tab. IX
	$p_{t,c,in}$	bar	13.5	32.0	25.9	-	-	25.9[e)]	[4] Fig. 13
	$T_{t,c,in}$	K	809	861	883.15	-	-	883.15	[4] Tab. IX
SAS Rotor 1	$\dot{m}_c$	kg/s	1.92[f)]	4.45[f)]	3.61[f)]	-	-	-	-
	$\dot{m}_{c,rel}$	%	6.09	6.09	6.09	-	-	-	-
	$\dot{m}_{c,rel,AF}$	%	3.30	3.30	3.30	-	-	3.30	[4] Fig. 24
	$\dot{m}_{c,rel,D}$	%	2.19	2.19	2.19	-	-	-	-
	$\dot{m}_{c,rel,Sh}$	%	0.60	0.60	0.60	-	-	0.60	[4] Tab. VII
	$p_{t,c,in}$	bar	13.9[g)]	32.8[g)]	26.6[g)]	-	-	-	-
	$T_{t,c,in}$	K	780	833	855.15	-	-	-	-
SAS Stator 2	$\dot{m}_c$	kg/s	0.43[f)]	0.99[f)]	0.80[f)]	-	-	-	-
	$\dot{m}_{c,rel}$	%	1.35	1.35	1.35	-	-	-	-
	$\dot{m}_{c,rel,AF}$	%	1.1	1.1	1.1	-	-	1.1	[4] Fig. 32
	$\dot{m}_{c,rel,PF}$	%	0.2	0.2	0.2	-	-	0.2	[4] Fig. 32
	$\dot{m}_{c,rel,L}$	%	0.05	0.05	0.05	-	-	0.05	[4] Fig. 32
	$p_{t,c,in}$	bar	7.1[g)]	17.1[g)]	14.1[g)]	-	-	-	-
	$T_{t,c,in}$	K	690	739	761.15	-	-	761.15	[4] Fig. 33

SAS Rotor 2	$\dot{m}_c$	kg/s	0.56	1.29	1.04	-	-	-	-
	$\dot{m}_{c,rel}$	%	1.76	1.76	1.76	-	-	-	-
	$\dot{m}_{c,rel,AF}$	%	0.76	0.76	0.76	-	-	0.76	[4] Fig. 34
	$\dot{m}_{c,rel,D}$	%	0.65	0.65	0.65	-	-	0.65[h)]	[4] Tab. VII [4] Fig. 32
	$\dot{m}_{c,rel,Sh}$	%	0.35	0.35	0.35	-	-	0.35	[4] page 59
	$p_{t,c,in}$	bar	7.1[g)]	17.1[g)]	14.1[g)]	-	-	-	-
	$T_{t,c,in}$	K	797	844	866.15	-	-	866.15	[4] page 54
Shaft	n	1/s	210.8	218.7	222.1	210.8[i)]	219.1[i)]	221.5	[4] Tab. I [4] Tab. VIII
	η_{mech}	-	0.9990	0.9990	0.9990	-	-	-	-

a) Mass flow is calculated using the parameter “Corrected Airflow” with T_{std} = 288.15 K and p_{std} = 101325 Pa.

b) Mass flow is calculated using the parameter “Corrected Flow $W\sqrt{T}/P$” with $W = W_{41}$, $T = T_{41}$, $P = P_4$ (see Tab. I of the HPT test report [20]). T_{41} is taken from Tab. 1 in the HPT design report [4], whereas P_4 is taken from the generated 0D performance model due to missing literature data.

c) η_{is} is defined as $\frac{h_{t,41,virt}-h_{t,415}}{h_{t,41,virt}-h_{t,415,is}}$ for two-stage turbines. In GTlab [15], multi-stage turbines are modeled as equivalent single-stage turbines [21, 22]. Stator 1 cooling air (non-chargeable) is ejected isobarically upstream of the equivalent single-stage rotor to calculate $T_{t,41}$. Additional non-chargeable cooling air of rotor 1 and stator 2 is ejected isobarically upstream of the equivalent single-stage rotor to calculate $T_{t,41,virt}$. Rotor 2 cooling air (chargeable) and chargeable cooling air of rotor 1 and stator 2 is ejected isobarically downstream of the equivalent single-stage rotor.

d) Cooled turbine efficiency definition is not known.

e) Average value between hub and tip cooling bleed.

f) According to the stage work distribution shown in Fig. 2 of the HPT design report [4], it is assumed that 56.5 % of the total coolant mass flow is chargeable and 43.5 % is non-chargeable.

g) No pressure loss considered within the SAS since no data is provided in the HPT design report [4].

h) Sum of the portions “Disk 2 Aft-Cavity Purge Air” in Tab. VII and “$w_{Seal\ Purge}$” in Fig. 32.

i) Rotational speed is calculated using the parameter “Speed $N\sqrt{T}$” with $T = T_{41}$ (see Tab. I of the HPT test report [20]). T_{41} is taken from Tab. 1 in the HPT design report [4].

Compressor map of GE's E3 HPC

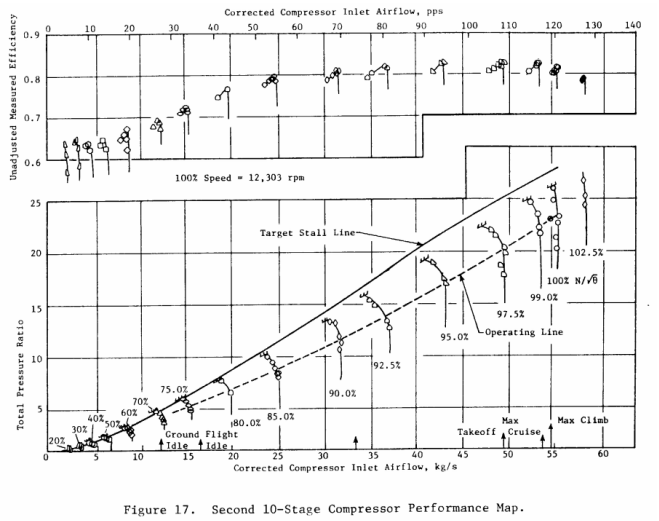

Figure 17. Second 10-Stage Compressor Performance Map.

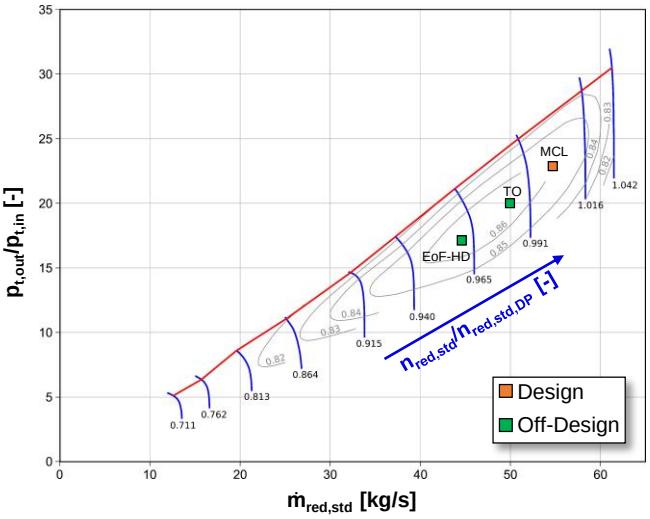

Original compressor map of GE's E3 HPC (left) taken from the HPC test report [18].